Monitoring the Earth's deformation with the SPOTGINS series

Alvaro Santamaría-Gómez^{1,2}, Jean-Paul Boy³, Florent Feriol¹, Médéric Gravelle⁴, Sylvain Loyer⁵, Samuel Nahmani^{6,7}, Joëlle Nicolas⁸, José Luis García Pallero⁹, Aurélie Panetier^{6,7}, Arnaud Pollet^{6,7}, Pierre Sakic⁶, Guy Wöppelmann⁴

- 5 ¹ Geosciences Environnement Toulouse, Université Paul Sabatier, CNES, CNRS, IRD, UPS, Toulouse, France.
 - ² Centre National d'Etudes Spatiales, Toulouse, France.
 - ³ Institut Terre-Environnement Strasbourg, Université de Strasbourg, ENGEES, Strasbourg, France.
 - ⁴ Littoral Environnement et Sociétés (LIENSs), CNRS, La Rochelle University, La Rochelle, France.
 - ⁵ Localisation & Orbitographie, Collecte Localisation Satellite, Ramonville Saint-Agne, France.
- 10 6 Université Paris Cité, Institut de physique du globe de Paris, CNRS, IGN, Paris, France.
 - ⁷ Université Gustave Eiffel, ENSG, IGN, Paris, France.
 - ⁸ Laboratoire Géomatique et Foncier, Cnam, Le Mans, France.
 - ⁹ ETSI en Topografía, Geodesia y Cartografía, Universidad Politécnica de Madrid, Madrid, Spain.

Correspondence to: Alvaro Santamaría-Gómez (alvaro.santamaria@cnes.fr)

- Abstract. A distributed Global Navigation Satellite System analysis center, designated SPOTGINS, has been established by several research groups that utilize the GINS software and the CNES-CLS precise products. Despite the heterogeneity in their research objectives, the SPOTGINS members apply the same configuration and metadata. The computed global ambiguity-fixed precise point positioning time series are fully consistent among the members, and are subsequently published as a single product. At the time of writing (August 2025), the SPOTGINS dataset includes 5768 daily series from May 2000 to present.
- This product facilitates a range of research activities, including but not limited to the precise monitoring of the Earth's deformation and the water vapor content of the troposphere. A comparison of the SPOTGINS series with published series from the Nevada Geodetic Laboratory solution shows no significant difference in quality.

1 Introduction

40

The Shared and Operational PPP Solutions Processed with GINS (SPOTGINS) is a novel initiative based on a distributed Global Navigation Satellite System (GNSS) analysis center where independent research groups cooperate by using the same software, the same processing strategy, and the same metadata to generate a common set of GNSS time series. The primary objective of this initiative is the generation of daily global Precise Point Positioning (PPP) position time series, as well as hourly zenith tropospheric delay (ZTD) time series. These series allow monitoring the Earth's deformation and the atmospheric water vapor content at the millimeter level through the 21st century. The latest and operational SPOTGINS position time series are currently available on The Geodesy Plotter of the Solid Earth Center portal (ForM@Ter)¹. The ZTD series will be available on the same portal in the near future.

The SPOTGINS cooperative was established in 2022 following the third reprocessing campaign of the International GNSS Service (IGS; Johnston et al., (2017)), when several research groups in France started to produce ambiguity-fixed GPS and Galileo PPP position time series with the GINS software (Michel et al., 2021; Nicolas et al., 2021), and the precise orbit, clock and phase biases computed by the Centre National d'Etudes Spatiales (CNES) - Collecte Localisation Satellites (CLS) IGS analysis center (Loyer et al., 2012). The research groups decided to unite into a collaborative processing effort with the support of the CNES-CLS analysis center. Each SPOTGINS member pursues distinct research objectives related to the Earth's deformation or the tropospheric water vapor, yet all contribute to the common processing by providing the series of a chosen set of GNSS stations depending on their geographic location, network label, or research project. By applying the same processing strategy, the obtained series are fully consistent and interchangeable among the members. At the time of writing (AprilAugust 2025), the current members are described in Table 1. Figure 1 illustrates the distribution of the SPOTGINS subnetworks processed by each member. The total number of stations is 5768 as of AprilAugust 2025.

The processing strategy is based on the zero-differenced ionosphere-free ambiguity-fixed carrier phase and code observations from the GPS and Galileo constellations. The models and corrections applied are described below and are fully consistent with the strategy used by the CNES-CLS IGS analysis center to compute the precise orbit and clock products. This avoids any relative range bias with respect to the fixed orbit and clock products, which increases the quality of the computed PPP series. Consequently, SPOTGINS can be regarded as the PPP densification of the CNES-CLS network solution aligned to the IGS20 reference frame (Rebischung et al., 2024).

In addition to a common processing strategy, the SPOTGINS members also share the station metadata. This metadata includes the following: station reference coordinates, receiver and antenna models, antenna eccentricity, antenna orientation, ocean tide loading coefficients, and co-seismic station displacement predictions from Métivier et al., (2014). The metadata concerning the history of the stations equipment and coordinates are also available in GINS format². Each member is responsible for providing the full history of each station's metadata, and also for keeping it up to date, within their respective sub-networks.

¹ https://www.poleterresolide.fr/geodesy-plotter-en/#/?solution=SPOTGINS (accessed April August 2025)

² https://ac-gnss.pagelab.univ-lr.fr/spotgins/www/station file.dat (accessed August 2025)

55 The consistency of the series computed by each member is periodically validated by the intercomparison of a small set of stations processed by all members.

Since our PPP series are fully consistent with the GNSS products used to generate them, the versioning of the SPOTGINS dataset is driven by the versioning of the CNES-CLS GNSS products. At this time, the version of the SPOTGINS dataset points to the G20/GRG products, which consists of the reprocessing made by CNES-CLS from May 2000 to January 2023 based on the IGS20 frame (G20 products), completed by the operational products since January 2023 (GRG products). The operational GRG products use the same strategy as the reprocessed G20 products, so both product labels can be used together. In case a new series of CNES-CLS GNSS products is available in the future, the SPOTGINS dataset will be updated with a new version.

Table 1. List of members participating in SPOTGINS in April August 2025.

Acronym	Member name				
EOST	Ecole et Observatoire des Sciences de La Terre, Institut Terre et Environnement de Strasbourg				
	https://eost.unistra.fr, https://ites.unistra.fr				
ESGT	Ecole Supérieure des Géomètres et Topographes, Laboratoire Géomatique et Foncier (GeF)				
	https://www.esgt.cnam.fr/recherche				
IPGP	Institut de Physique du Globe de Paris				
iror	https://www.ipgp.fr/en				
OMP	Observatoire Midi-Pyrénées, Géosciences Environnement Toulouse				
	https://www.get.omp.eu				
ULR	Université de La Rochelle, Littoral Environnement Sociétés				
	https://lienss.univ-larochelle.fr				
UPM	Universidad Politécnica de Madrid, Escuela Técnica Superior de Ingenieros en Topografía,				
	Geodesia y Cartografía				
	https://www.topografia.upm.es				

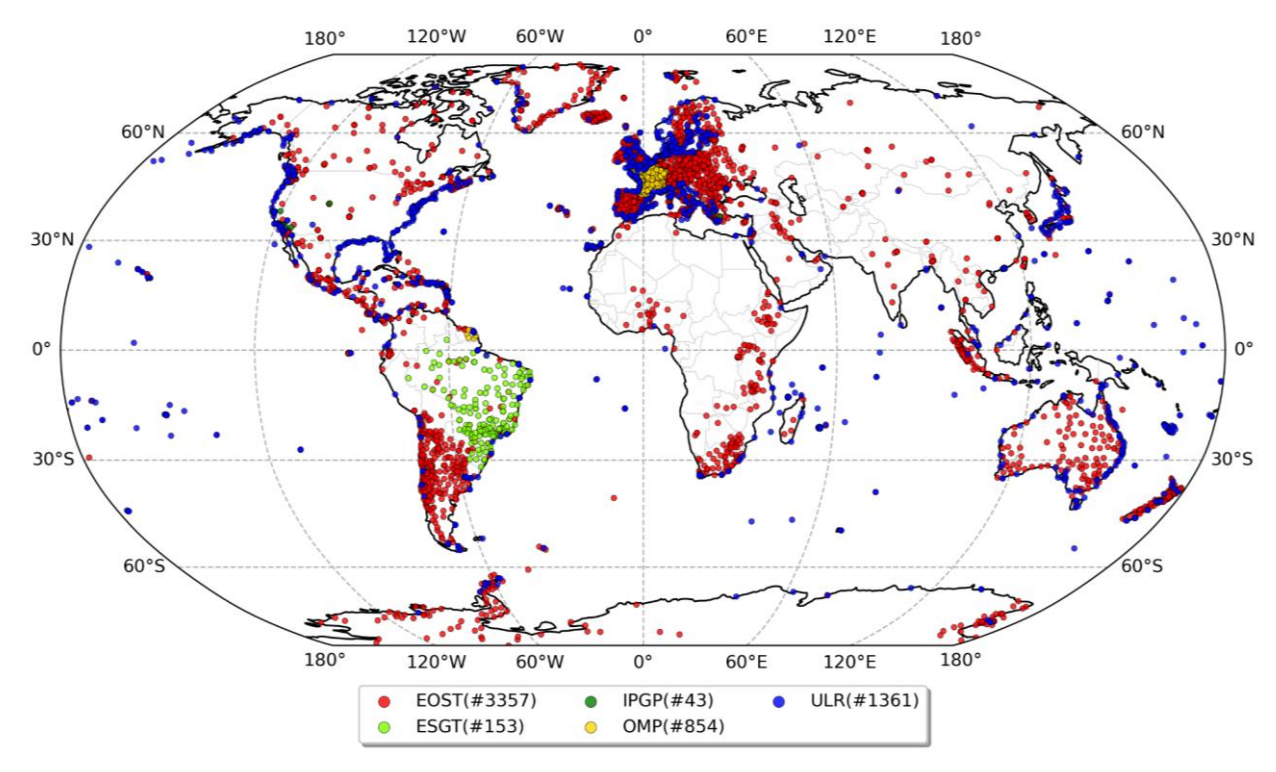


Figure 1: The SPOTGINS sub-networks processed by each member in April August 2025. The number of stations included in each sub-network is also indicated.

70 2 GNSS data processing

The PPP processing is based on ambiguity-fixed carrier phase and code observations from the GPS constellation, since mMay 2000, and the Galileo constellation, since October 2018. These dates correspond to the availability of the ambiguity-fixed CNES-CLS precise products for each constellation. The observations are sampled at 5 min, and a cut-off elevation angle of 8 degrees is applied to minimize errors caused by multipath, atmospheric propagation, and receiver/satellite antenna phase patterns. The a priori station coordinates are obtained from the shared metadata and only loose constraints are applied to the parameter estimates.

The input observations are screened for quality and their uncertainty (s) is assigned by ana fixed empirical elevation-dependent (e) function based on stacked long termcumulated post-fit residuals. This function takes the following form:

$$S = \frac{S_0}{a + (1 - a)\sin(e)} \tag{1}$$

where S_0 is the observation uncertainty at the zenith with values of 3.5 mm and 600 mm for phase and code observations, respectively, and a is the amplification term with a value of 0.15, which accounts for the increase in the observations variance

<u>at low elevation</u>. The elevation-dependent uncertainties obtained are then scaled <u>each day</u> by the relative precision of the computed orbit for each individual satellite.

Phase observations are corrected for wide-lane satellite-dependent biases computed weekly by the CNES-CLS analysis center³, which, together with the associated daily integer satellite phase clock biases, allow PPP users to perform ionosphere-free integer ambiguity resolution for each GNSS station (Laurichesse et al., 2009). Similarly, to comply with the GPS P1/P2 convention of the IGS products, code observations are corrected, when necessary, for satellite-dependent monthly differential code biases computed by the Centre for Orbit Determination in Europe.

Satellite-dependent antenna phase center offsets (PCO) in the nadir direction and block-dependent horizontal PCO corrections are applied using the IGS20 antenna calibration model. Satellite block-dependent nadir angle-dependent absolute phase center variations (PCV) are corrected using the same IGS20 model. For the receiver antenna, absolute PCO and direction-dependent PCV corrections are also applied using the IGS20 model. All PCO and PCV corrections are frequency-dependent. The receiver antenna PCO/PCV corrections are rotated according to the antenna orientation indicated in each station's sitelog file.

Phase observations are corrected for the wind-up effect (Wu et al., 1993) by taking into account the satellite attitude using the nominal yaw model for GPS (Bar-Sever, 1996), and the nominal attitude law for Galileo released by the EU Agency for the Space Programme (EUSPA)⁴. The CNES-CLS satellite clocks are corrected for second-order relativistic effects due to the small orbit ellipticity of the GPS satellites. The receiver's clock phase bias is estimated on an epoch-by-epoch basis with no constraints. Furthermore, a daily receiver clock phase bias is removed between the GPS and Galileo observations.

Signal path delays due to the propagation through the neutral atmosphere are corrected using the VMF1 mapping function grids (Boehm et al., 2006), which include zenith hydrostatic and wet delays <u>estimated</u> from the European Centre for Medium-Range Weather Forecasts (ECMWF) <u>ERA-40</u> reanalysis <u>and operational products</u>. The zenith wet delays are adjusted using a piecewise linear function at 1-hour intervals, together with two horizontal gradients per day (Chen and Herring, 1997).

Signal path delays due to the propagation through the ionosphere are accounted for, at first-order, by forming the ionosphere-free linear combination of the L1/L2 GPS and the E1/E5a Galileo frequencies. Second-order ionospheric delays are corrected using the vertical total electron content values extracted from the daily IGS Final Global Ionosphere Maps (Hernández-Pajares et al., 2011).

Station displacements due to the solid Earth, solid Earth pole, and ocean pole tides are corrected using the 2010 International Earth Rotation and Reference Systems Service conventions (Petit and Luzum, 2010), including the latest linear mean pole model. The solid Earth tide correction also includes the permanent term, which corresponds to a conventional tide-free frame. Station displacements due to ocean tide loading are corrected using predictions for the 11 main tidal constituents extracted from the FES2014b (Lyard et al., 2021) modeland with respect to a center-of-figure (CF) frame, which are then completed by

90

100

105

110

³ <u>https://igsac-cnes.cls.fr/html/products.html</u> (accessed <u>April August</u> 2025)

⁴ https://www.gsc-europa.eu/support-to-developers/galileo-satellite-metadata (accessed April August 2025)

interpolating the tidal admittances. Displacements due to the atmospheric thermal tides loading and the non-tidal loadings are not corrected at the observation level.

A summary of the SPOTGINS processing strategy is available at the Solid Earth Center portal (ForM@Ter)⁵. This file may change in the future to reflect changes in the processing strategy with respect to the description given above.

3 Comparison of the SPOTGINS series

120

125

130

The SPOTGINS position time series have been compared to published series from the Nevada Geodetic Laboratory (NGL; Blewitt et al., 2018). The NGL is a global PPP solution obtained with the Gipsy software and the JPL IGS precise products-based on the IGb14 frame. Figure 2 shows an example of the difference of position time series obtained from these two solutions for the same station. The ITRF2020 plate motion model (Altamimi et al., 2023) was removed from both solutions for visualization purposes. The vertical jump near 2019 is here likely caused by the use of wrong station metadata in the NGL solution. Position offsets like this, affecting mostly the vertical component, are typically caused by wrong metadata and antenna changes. There is no change in our metadata, nor in the header of the RINEX files we use, and unfortunately, we lack of enough information to explain the offset in the series of the NGL solution. The apparent drifts in the E and U components may be explained by several factors, including the differences of the reference frame (IGS14 vs IGS20) and the way each solution realizes their reference frame, but also differences in the processing software and in the GNSS products. Small drifts may exist, but also small position offsets that may be interpreted as a drift.

Fig. The3 shows the dispersion of the detrended and cleaned series by solution and coordinate component is shown in for 2948 Fig. 3, together with the number of common stations, between both solutions. The same period was considered for each of the 2948 pairs of common stations considered. The typical dispersion of both the SPOTGINS and NGL solutions is at the level of 2 mm and 6 mm, for the horizontal and vertical components, respectively.

⁵ https://www.poleterresolide.fr/geodesy-plotter-en/#/solution/SPOTGINS (accessed April August 2025)

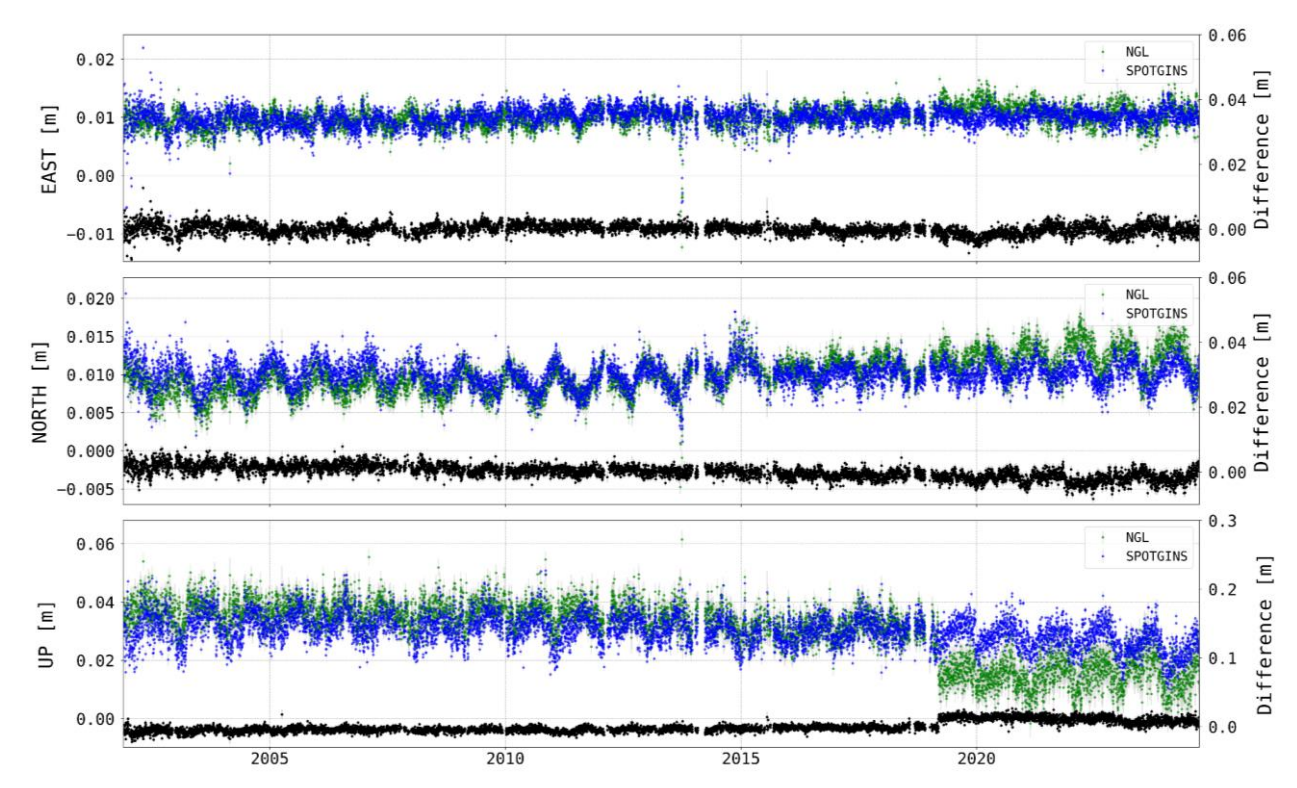
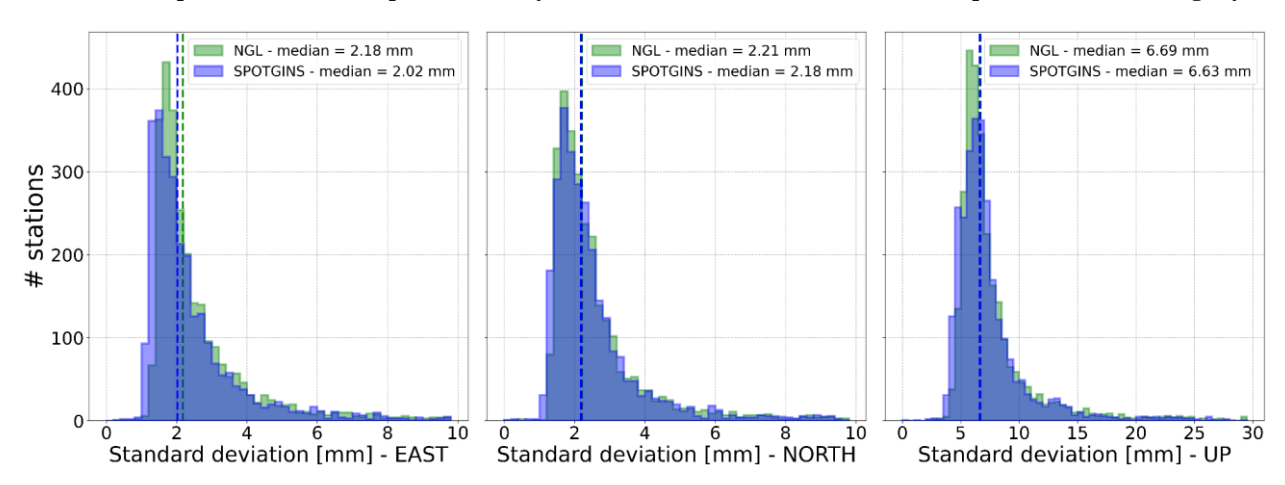


Figure 2: Time series of daily displacements from the SPOTGINS (in blue) and NGL (in green) solutions for the LROC00FRA station with respect to the Eurasian plate. The daily differences between both solutions are represented in black (right y-axis).



135

140

Figure 3: TimeComparison of the scatter of the detrended and cleaned position series of daily displacements from between the SPOTGINS (in-blue) and the NGL (in-green) solutions for the LROC00FRA station with respect to the Eurasian plate. The daily differences between both solutions are represented in blackeast (left), north (center) and up (right y-axis), coordinate components.

To assess the quality of the terrestrial frame realized by the SPOTGINS position series, we compared the terrestrial frame defined by the estimated positions of 410 IGS stations included in the SPOTGINS solution, day by day, to the ITRF2020 reference frame. We estimated the daily translations, rotations and scaling factors between the SPOTGINS solution and the

ITRF2020. As the CNES-CLS orbit and clock products used to compute the SPOTGINS solution are referenced to the IGS20 frame, the obtained SPOTGINS series must also be referenced to the ITRF2020 frame, i.e. no net translation, rotation and scale change should exist between both frames. Small departures from the ITRF2020 are expected due to the different number of stations used in alignment of the CNES-CLS products, which varies with time.

145

Figure 4 shows the estimated time series of the daily transformation parameters and the number of stations used in the alignment. The mean bias and drift of each transformation parameter are shown in Table 2. All transformation biases and drifts are smaller than 1 mm and 0.1 mm/year, respectively, confirming the excellent quality of the referencing of the SPOTGINS solution.

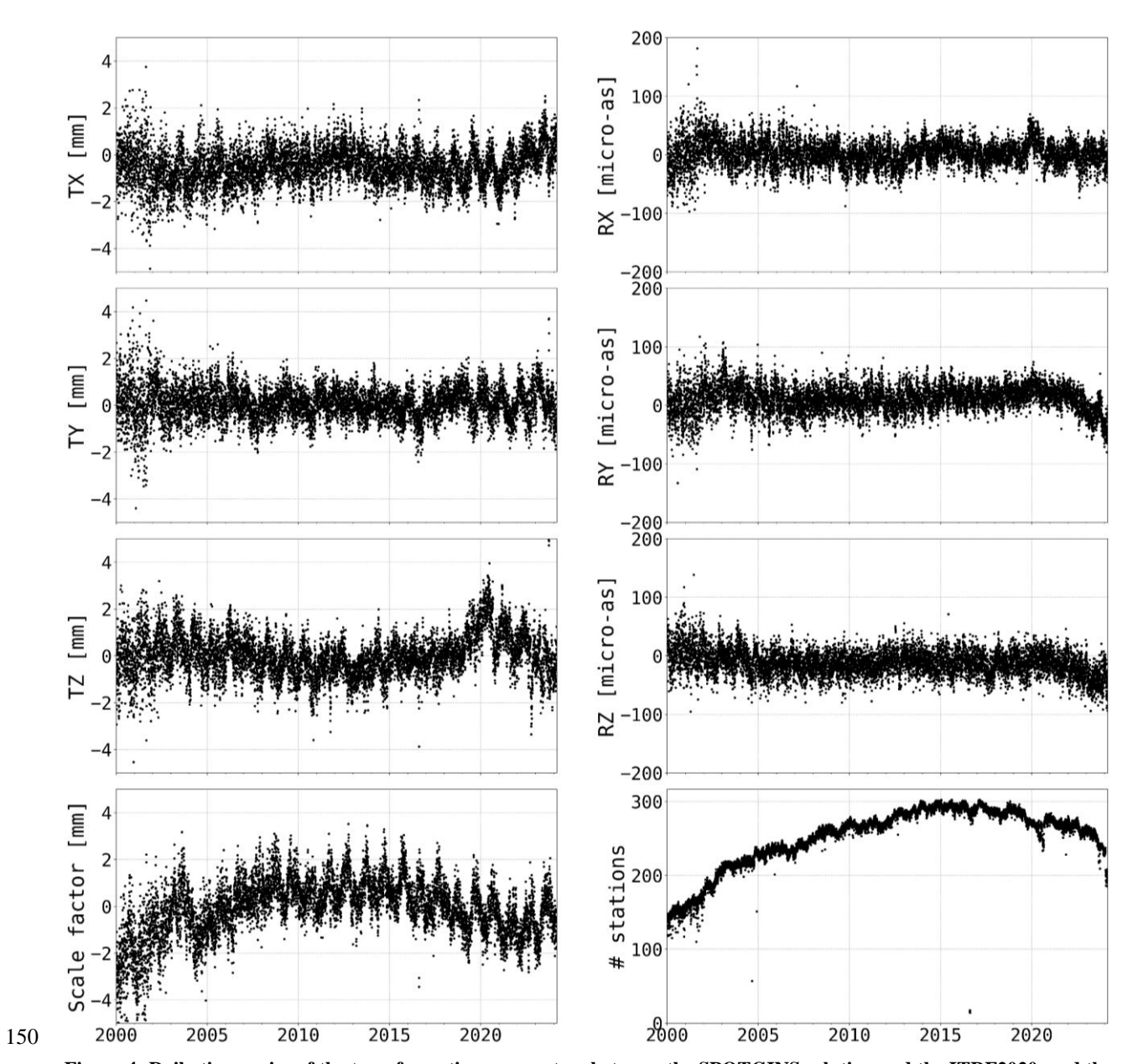


Figure 4: Daily time series of the transformation parameters between the SPOTGINS solution and the ITRF2020, and the number of common stations used for the computation. Translation and scale factor in millimeters, rotation in micro-arc seconds.

Table 2. Bias and drift of the transformation parameters between the SPOTGINS solution and the ITRF2020.

	TX (mm)	TY (mm)	TZ (mm)	SC (mm)	RX (mm)	RY (mm)	RZ (mm)
Bias	-0.54 +/- 0.01	0.08 +/- 0.01	-0.01 +/- 0.01	0.02 +/- 0.01	0.09 +/- 0.01	0.38 +/- 0.01	-0.31 +/- 0.01
Drift	0.01 +/- 0.00	0.00 +/- 0.00	0.01 +/- 0.00	0.08 +/- 0.00	0.00 +/- 0.00	0.02 +/- 0.00	-0.02 +/- 0.00

Data availability

155

160

165

170

175

180

The <u>operational</u> SPOTGINS position time series are available from ForM@Ter, the French National Solid Earth Center portal (https://www.poleterresolide.fr/geodesy-plotter-en/#/?solution=SPOTGINS, accessed https://doi.org/10.24400/170160/20250414 (Santamaría-Gómez et al., 2025).

The GNSS data used to compute the SPOTGINS series are available from the data servers included in the supplemental material. following data servers: Agency for Data Supply and Infrastructure (SDFI), Agenzia Spaziale Italiana (ASI), British Geological Survey (BGS), Bundesanstalt für Gewässerkunde (BAFG), Cartográfica de Canarias, S.A. (GRAFCAN), Centre d'Etudes Alexandrines (CEAlex), Comunidad Autonoma de la Region de Murcia (CARM), Delft University of Technology (TUDELFT) doi: 10.4121/9CD4ED76-F374-4737-BE01-0ADC927550E2, Departamento de Geofísica, Centro Sismologico Nacional, Univ. de Chile (DGF-CSN), Deutsches GeoForschungsZentrum (GFZ) doi: 10.5880/GFZ.1.1.2020.001, Digitaal Vlaanderen (DV) doi: 10.24414/ROB-FLEPOS, Diputacion Foral de Vizcaya (DFV), Direction des Infrastructures, de la Topographie et des Transports Terrestres (DITTT/BANIAN), EPOS-FR / Réseau National GNSS Permanent (RENAG) doi: 10.15778/RESIF.RG, EUREF Permanent GNSS Network (EUREF), Estonian Land Board (ELB), European Plate Observatory System (EPOS), European Space Agency (ESA), Geodata Diffusion (ORPHEON) doi: 10.15778/RESIF.RG, Geoscience Australia (GA), Geospatial Information Authority of Japan (GSI), Institut Cartografic i Geologic de Catalunya (ICGC), Institut Cartogràfic Valencià (ICV), Institute of Geodynamics (GEIN-NOA), Institute of Geological and Nuclear Sciences Limited (GNS) doi: 10.21420/RXKE-AZ44, Instituto Brasileiro de Geografia e Estatística (IBGE), Instituto Espanol de Oceanografia (IEO), Instituto Geografica Nacional de la Republica Argentina (IGNRA), Instituto Geografico Agustin Codazzi (IGAC), Instituto Geografico Militar Ecuador (IGM EC), Instituto Geografico Militar Uruguay (IGM UR), Instituto Geografico Nacional (IGNE), Instituto Geografico Nacional Tommy Guardia (IGNTG), Instituto Geografico de Aragon (IGEAR), Instituto Nacional de Estadística y Geografía (INEGI), Instituto Nacionale de Oceanografía e di Geofisica Sperimentale (INOGS), Instituto Tecnologico Agrario de Castilla y Leon (ITACYL), Instituto de Estadística y Cartografía de Andalucía (IECA), Instituto de Geofísica - Servicio Mareográfico Nacional - UNAM (SMN-UNAM), International GNSS Service (IGS), International Laser Ranging Service (ILRS), Istituto Nazionale di Geofisica e Volcanologia (INGV) doi: 10.13127/RING,

Japan Aerospace Exploration Agency (JAXA), Kadaster (NSGI), Korea Astronomy and Space Science Institute (KASI), LIttoral ENvironnement et Sociétés (LIENSs-OASU) doi: 10.60888/EPOS-GNSS-SONEL-NODE, La Rete GPS Veneto (RETE GPS VENETO), La Rochelle University (ULR) doi: 10.60888/EPOS-GNSS-SONEL-NODE, Laboratoire de Géologie de l'Ecole normale supérieure (GEOL-ENS), Lands Department - Hong-Kong (LD-HK), Latvijas Geotelpiskas 185 Informacijas Agentura (LGIA LatPOS), Marine Institute (MI), NERC British Isles continuous GNSS Facility (BIGF), NERC Space Geodesy Facility (NSGF), National Geo-Spatial Information (NGI), National Institute for Earth Physics (NIEP), National Oceanic and Atmospheric Administration (NOAA), National Oceanography Centre (NOC), National Resources Canada (NRCan), Northern California Earthquake Data Center (NCEDC) doi: 10.7932/NCEDC, Norwegian Mapping Authority - Kartverket (NMA), Ordnance Survey Geodesy and Positioning (OS), Ordnance Survey Ireland (OSI), Polish Polar 190 Station, Hornsund (PPS), Regione Campania (RC), Rete Dinamica Nazionale (RDN), Royal Observatory of Belgium (ROB) doi: 10.24414/FST8-P256, Réseau GNSS Permanent (IGN/RGP), SWEPOS Lantmäteriet (SWEPOS-LMV) doi: 10.23701/c5tc-ew52, Satellite Positioning Service (SAPOS), SONEL doi: 10.60888/EPOS-GNSS-SONEL-NODE, The Canadian High Arctic Ionospheric Network (CHAIN) doi: 10.1029/2008RS004046, The Hartebeesthoek Radio Astronomy Observatory (HartRAO) doi: 10.5281/ZENODO.10996, Universidade da Beira Interior (UBI) doi: 10.25768/ubi-epos-gnss-195 pt, University NAVSTAR Consortium / GAGE (UNAVCO), University of California, San Diego (UCSD), University of Hawai'i Sea Level Centre (UHSLC), Volcanological and Seismological Observatories of the Institut de Physique du Globe de Paris (IPGP-OVS) (VOLOBSIS), Western Canada Deformation Array (WCDA) doi: 10.7914/zw3f-h051, Wuhan University (WHU).

The ORPHEON GNSS RINEX data are provided for scientific use in the framework of the GEODATA-INSU-CNRS convention.

Author contributions

ASG, JPB, FF, MG, SL, SN, JN, APa, APo and PS processed the GNSS data. SL provided technical support with the GINS software and the CNES-CLS precise products. MG provided the results of the comparison analysis. APo provided the results of the alignment analysis. ASG wrote the manuscript with corrections provided by FF, MG, SL, JN, JLPG, APo and PS. MG created the figures.

Competing interests

205

The authors declare that they have no conflict of interest.

Acknowledgements

The authors are thankful to the CNES and CLS space geodesy teams for their support with the GINS software, and to Elisabeth Pointal and the Geodesy Plotter team for their support with the publication of the series. All the past, present and future members of SPOTGINS are acknowledged for their past, present and future contributions to this cooperative effort. Especially, Alexandre Michel is acknowledged for developing the initial file structure, the name and logo of SPOTGINS and the name of SPOTGINS. The authors would also like to acknowledge Thierry Guyot (LIENSs, La Rochelle University) for designing the SPOTGINS logo.

215

220

Financial support

SPOTGINS is financially supported by CNES as an application of the IGS-AC, DEFRHEO, and GEOSPARC projects. IPGP's processing is performed on the S-CAPAD/DANTE numerical computations platform. The GNSS processing of the coastal stations by ULR has been supported by the SONEL observing system (ILICO Research Infrastructure) and by the French State under the PPR FUTURISKS Project, 'Un Océan de Solutions', managed by the National Research Agency, under France 2030 [grant No.ANR-22-POCE-0002]. J.L.G. Pallero acknowledges the support of the Universidad Politécnica de Madrid through a Programa Propio de Movilidad grant for a research stay in Toulouse in 2025.

References

- Altamimi, Z., Métivier, L., Rebischung, P., Collilieux, X., Chanard, K., Barnéoud, J., 2023. ITRF2020 Plate Motion Model. Geophys. Res. Lett. 50, e2023GL106373. https://doi.org/10.1029/2023GL106373
 Bar-Sever, Y.E., 1996. A new model for GPS yaw attitude. J. Geod. 70, 714–723. https://doi.org/10.1007/BF00867149
 Blewitt, G., Hammond, W.C., Kreemer, C., 2018. Harnessing the GPS data explosion for interdisciplinary science. EOS 99.
 - https://doi.org/10.1029/2018EO104623

 Boehm, J., Werl, B., Schuh, H., 2006, Troposphere mapping functions for GPS and very long baseline interferometry from
- Boehm, J., Werl, B., Schuh, H., 2006. Troposphere mapping functions for GPS and very long baseline interferometry from European Centre for Medium-Range Weather Forecasts operational analysis data. J. Geophys. Res. Solid Earth 111, B02406. https://doi.org/10.1029/2005JB003629
 - Chen, G., Herring, T.A., 1997. Effects of atmospheric azimuthal asymmetry on the analysis of space geodetic data. J. Geophys. Res. Solid Earth 102, 20489–20502. https://doi.org/10.1029/97JB01739
- Hernández-Pajares, M., Juan, J.M., Sanz, J., Aragón-Àngel, À., García-Rigo, A., Salazar, D., Escudero, M., 2011. The ionosphere: effects, GPS modeling and the benefits for space geodetic techniques. J. Geod. 85, 887–907. https://doi.org/10.1007/s00190-011-0508-5

Johnston, G., Riddell, A., Hausler, G., 2017. The International GNSS Service, in: Teunissen, P.J.G., Montenbruck, O. (Eds.), Springer Handbook of Global Navigation Satellite Systems. Springer International Publishing, Cham, pp. 967–982. https://doi.org/10.1007/978-3-319-42928-1 33

240

245

- Laurichesse, D., Mercier, F., Berthias, J.-P., Broca, P., Cerri, L., 2009. Integer Ambiguity Resolution on Undifferenced GPS Phase Measurements and Its Application to PPP and Satellite Precise Orbit Determination. Navigation 56, 135–149. https://doi.org/10.1002/j.2161-4296.2009.tb01750.x
- Loyer, S., Perosanz, F., Mercier, F., Capdeville, H., Marty, J.-C., 2012. Zero-difference GPS ambiguity resolution at CNES-
- Lyard, F.H., Allain, D.J., Cancet, M., Carrère, L., Picot, N., 2021. FES2014 global ocean tide atlas: design and performance.

 Ocean Sci. 17, 615–649. https://doi.org/10.5194/os-17-615-2021

CLS IGS Analysis Center, J. Geod. 86, 991–1003. https://doi.org/10.1007/s00190-012-0559-2

- Métivier, L., Collilieux, X., Lercier, D., Altamimi, Z., Beauducel, F., 2014. Global coseismic deformations, GNSS time series analysis, and earthquake scaling laws. J. Geophys. Res. Solid Earth 119, 9095–9109. https://doi.org/10.1002/2014JB011280
- Michel, A., Santamaría-Gómez, A., Boy, J.-P., Perosanz, F., Loyer, S., 2021. Analysis of GNSS Displacements in Europe and Their Comparison with Hydrological Loading Models. Remote Sens. 13, 4523. https://doi.org/10.3390/rs13224523
 Nicolas, J., Verdun, J., Boy, J.-P., Bonhomme, L., Asri, A., Corbeau, A., Berthier, A., Durand, F., Clarke, P., 2021. Improved Hydrological Loading Models in South America: Analysis of GPS Displacements Using M-SSA. Remote Sens. 13. https://doi.org/10.3390/rs13091605
- Petit, G., Luzum, B., 2010. IERS Conventions, IERS Technical Note 36. Frankfurt am Main: Verlag des Bundesamts für Kartographie und Geodäsie.
 - Rebischung, P., Altamimi, Z., Métivier, L., Collilieux, X., Gobron, K., Chanard, K., 2024. Analysis of the IGS contribution to ITRF2020. J. Geod. 98, 49. https://doi.org/10.1007/s00190-024-01870-1
 - Santamaría-Gómez, A., Boy, J.-P., Feriol, F., Gravelle, M., Loyer, S., Nahmani, S., Nicolas, J., García Pallero, J.L., Panetier,
- 260 A., Pollet, A., Sakic, P., 2025. SPOTGINS GNSS position and tropospheric delay series. https://doi.org/10.24400/170160/20250414
 - Wu, J.T., Wu, S.C., Hajj, G.A., Bertiger, W.I., Lichten, S.M., 1993. Effects of antenna orientation on GPS carrier phase. Manuscripta Geod. 18, 91–98.